

Article

Fabrication and Dry-Sliding Wear Characterization of Open-Cell AlSn6Cu–Al₂O₃ Composites with LSTM-Based Coefficient of Friction Prediction

Mihail Kolev ^{1,*} , Ludmil Drenchev ¹ , Veselin Petkov ¹, Rositza Dimitrova ¹ , Krasimir Kolev ¹  and Tatiana Simeonova ^{1,2}

¹ Institute of Metal Science, Equipment and Technologies with Center for Hydro- and Aerodynamics “Acad. A. Balevski”, Bulgarian Academy of Sciences, 1574 Sofia, Bulgaria; ljudmil.d@ims.bas.bg (L.D.); veselin.petkov@ims.bas.bg (V.P.); rossy@ims.bas.bg (R.D.); kkolev@ims.bas.bg (K.K.); tsimeonova@imbm.bas.bg (T.S.)

² Institute of Mechanics, Bulgarian Academy of Sciences, 1113 Sofia, Bulgaria

* Correspondence: mihailkolev@ims.bas.bg

Abstract: This study investigates the fabrication, wear characterization, and coefficient of friction (COF) prediction of open-cell AlSn6Cu–Al₂O₃ composites obtained by a liquid-state processing technique. Focusing on wear behavior under varying loads using the pin-on-disk method, this research characterizes microstructure and phase composition via SEM, EDS, and XRD analyses. A novel aspect of this research is the application of an LSTM recurrent neural network model for the fast and accurate prediction of the COF of the composites, eliminating the need for extensive experimental work. Additionally, feature importance analysis using Random Forest regressors is conducted to ascertain the relative contribution of each input variable to the output variable, enhancing our understanding of the wear mechanisms in these materials. The results demonstrate the effectiveness of the composite’s reinforcement in improving wear resistance, highlighting the critical role of mechanical stress and the reinforcement’s hardness in the wear process. The quantitative findings related to the wear behavior include a mass-wear reduction in the open-cell AlSn6Cu–Al₂O₃ composite from 8.05 mg to 1.90 mg at 50 N and a decrease from 17.55 mg to 8.10 mg at 100 N, demonstrating the Al₂O₃ particles’ effectiveness in improving wear resistance under different loads.

Keywords: Al-based metal matrix composites; AlSn6Cu–Al₂O₃; dry-sliding friction; wear behavior; long short-term memory model



Citation: Kolev, M.; Drenchev, L.; Petkov, V.; Dimitrova, R.; Kolev, K.; Simeonova, T. Fabrication and Dry-Sliding Wear Characterization of Open-Cell AlSn6Cu–Al₂O₃ Composites with LSTM-Based Coefficient of Friction Prediction. *Metals* **2024**, *14*, 428. <https://doi.org/10.3390/met14040428>

Academic Editor: Manoj Gupta

Received: 9 March 2024

Revised: 30 March 2024

Accepted: 3 April 2024

Published: 5 April 2024



Copyright: © 2024 by the authors. Licensee MDPI, Basel, Switzerland. This article is an open access article distributed under the terms and conditions of the Creative Commons Attribution (CC BY) license (<https://creativecommons.org/licenses/by/4.0/>).

1. Introduction

Aluminum-based metal matrix composites (AMMCs) are a notable innovation in the field of materials science, providing an optimal balance of reduced weight and improved mechanical robustness. These composites are particularly valued for their wear resistance, making them ideal for applications in sectors demanding high performance and durability, such as the automotive, aerospace, and defense industries [1,2]. The integration of aluminum alloys with various reinforcements, including ceramic particles or fibers, and the development of open-cell structures lead to materials that exhibit superior properties compared to their base metals. These properties include improved stiffness, strength, thermal stability, and enhanced thermal management and energy absorption capabilities, which are critical for specific applications [3,4].

Open-cell AMMCs, with their interconnected porosity, offer unique advantages such as improved energy absorption, which is crucial for impact resistance in automotive and aerospace applications [5]. The porous structure also facilitates better thermal management through enhanced heat dissipation, addressing one of the critical challenges in high-performance engineering applications [6,7].

Despite their numerous advantages, AMMCs, including those with open-cell structures, face several challenges that limit their widespread adoption. One of the main issues is their poor machinability, which complicates the manufacturing process and increases production costs [8,9]. The high cost of raw materials and processing poses a significant barrier to their use in cost-sensitive applications [10]. Additionally, difficulties in joining AMMCs with other materials can restrict their application in complex assemblies [11,12]. These challenges necessitate the development of new composite materials and processing techniques that can overcome these limitations while retaining or enhancing the desirable properties of AMMCs [5].

The exploration of open-cell AMMCs signifies a promising direction for overcoming the limitations of traditional AMMCs. By leveraging the inherent benefits of open-cell structures, researchers and engineers can develop composites that not only meet the high-performance criteria of demanding sectors but also offer solutions to the existing challenges of machinability, cost, and material integration [13–15].

Consequently, amidst these considerations and advances within the realm of AMMCs, the exploration of sintered aluminum–tin (Al–Sn) composites has emerged as a promising avenue for enhancing the understanding of wear mechanisms and improving the wear properties of AMMCs. Recent studies have illuminated the profound impact of alloying elements and processing methods on the wear resistance and mechanical characteristics of these composites under dry friction conditions.

For instance, the inclusion of tin-insoluble elements such as zinc (Zn) and silicon (Si) has been explored to bolster the tribotechnical and mechanical performance of Al–40Sn composites. Notably, sintering above the melting point of tin can introduce residual porosity that detrimentally affects strength, ductility, and wear resistance, whereas techniques like hot pressing and equal-channel angular pressing (ECAP) have shown potential to enhance these properties by diminishing porosity. Zinc-alloyed matrices, in particular, have exhibited superior wear resistance compared to their silicon-alloyed counterparts, underscoring the nuanced interplay between alloying elements and wear properties [16]. Further investigations have also demonstrated the strategic alloying of the aluminum matrix with zinc in Al–Sn alloys to improve yield strength and wear resistance, though the advantages become less pronounced under elevated pressures, revealing the complexity of wear mechanisms in these composites [17]. Additional studies incorporating Al₃Fe particles into Al–Sn composites through liquid-phase sintering and pressing have achieved consistent strength and enhanced wear resistance across varying sintering temperatures [18]. Comparative analyses suggest that prefabricated Al₃Fe particles more effectively contribute to the mechanical properties and wear resistance of Al–Sn–Fe alloys compared to pure iron powders, proposing a strategic approach to composite design [19]. Furthermore, research into directionally solidified Al–Sn–Cu and Al–Sn–Si alloys has shed light on the relationship between microstructure and tribological properties, indicating that finer microstructures in Al–Sn–Si alloys lead to increased tensile strength and potentially improved wear properties [20]. This body of research collectively advances our comprehension of wear behavior in Al–Sn composites and, by extension, AMMCs, offering valuable insights into optimizing their wear properties for engineering applications.

Building on the comprehensive overview of AMMCs and their significance in various high-demand sectors due to their enhanced wear resistance and mechanical properties, the integration of machine learning (ML) techniques in the prediction and optimization of these properties represents a cutting-edge progression in materials science. The recent advent of artificial intelligence (AI) methodologies, particularly ML, has opened new avenues for the design, analysis, and prediction of AMMCs' wear characteristics with unprecedented accuracy and efficiency.

Banerjee et al. [21] pioneered the application of artificial neural networks (ANN) for designing alumina-reinforced AMMCs, showcasing multi-objective optimization using genetic algorithms based on ANN models. This approach enables the tailored design of composites with optimized tribomechanical properties, marking a significant leap forward

in material science by integrating computational intelligence in materials design. Similarly, Wang et al. [22] explored the broader application of deep neural network learning in composite material systems design. Their review underscores the self-learning capabilities of deep learning models and highlights the necessity for well-constructed AI algorithms in predicting the behavior of modern composite materials, including AMMCs. Thankachan et al. [23] further demonstrated the utility of neural network models in predicting the material removal rate and surface roughness in wire electrical discharge machining of novel Al alloys and MMCs. The effectiveness of these models exemplifies the precision and adaptability of AI in fine-tuning manufacturing processes for enhanced material properties. Idrisi et al. [24] focused on the wear performance analysis of AA5083-SiC micro- and nanocomposites using ANN. Their study evaluates the model's performance and prediction capability, showcasing ANN's potential in accurately forecasting wear characteristics of reinforced AMMCs. Wiciak-Pikuła et al. [25] developed multilayer perceptron models using vibration acceleration and cutting force data to predict tool wear during the milling of AMMCs reinforced with SiC. This research highlights the effectiveness of ANN in predicting tool wear, offering a novel approach to monitoring and optimizing machining processes. Mishra et al. [26] presented an algorithm based on neurosymbolic artificial intelligence for predicting wear behavior in AMMCs reinforced with SiC. Their findings indicate superior performance over traditional ANN models, emphasizing the potential of integrating symbolic reasoning with neural learning for enhanced predictive accuracy. Agme et al. [27] utilized ANN and Taguchi optimization for analyzing and predicting the wear characteristics of sustainable MMCs. Their study demonstrates a 100% prediction accuracy, showcasing the powerful synergy between machine learning and decision-making algorithms in optimizing material properties. Lastly, Hasan et al. [28] applied various ML algorithms to model dry friction and wear of Al-based alloys. Their comparative analysis reveals that Random Forest (RF) and K-Nearest Neighbor (KNN) algorithms exhibit the best performance in predicting wear rates and coefficients of friction, respectively, illustrating the diverse potential of ML techniques in tribological studies.

The advancement of AMMCs has seen significant progress, particularly through the integration of ML for design and optimization. However, a notable research gap exists in the empirical validation of these predictive models, especially concerning the fabrication and testing of novel composites like open-cell AlSn6Cu-Al₂O₃. Despite the promising potential of these composites, there is limited empirical research focusing on their practical application. The fabrication of open-cell AlSn6Cu-Al₂O₃ composites using liquid-state processing techniques and their wear behavior analysis under various loads using the pin-on-disk method are crucial areas that require further exploration. Additionally, employing advanced ML models, such as Long Short-Term Memory (LSTM) networks for predicting the coefficient of friction (COF) offers a novel approach to enhancing prediction efficiency and accuracy, highlighting the need for a link between computational predictions and practical application in the development of AMMCs.

To address these issues, this research aims to fabricate open-cell AlSn6Cu-Al₂O₃ composites utilizing the liquid-state processing technique and assess the wear characteristics of the composites under varying loads through the pin-on-disk test method. The investigation into the composites will involve characterizing phase constituents and microstructural attributes through X-ray diffraction (XRD) patterns, energy-dispersive X-ray spectroscopy (EDS) analysis, and scanning electron microscopy (SEM) imaging. The COF of the composites will be predicted by a LSTM recurrent neural network model. This approach will provide a fast and accurate way to estimate the COF of the composites for any given combination of the input variables, without the need for additional experiments. Moreover, feature importance analysis will be conducted to predict the mass wear and COF of the composites and unreinforced materials using RF regressors, which will reveal the relative contribution of each input variable to the output variable. This study aims to significantly contribute to the field of materials engineering by developing wear-resistant AMMCs, serving as a continuation of previous research conducted on the subject. By integrating

computational predictions with empirical validations, it seeks to bridge existing gaps in the understanding and application of advanced composite materials. This research extends the findings of a prior study on open-cell AlSn6Cu composites, which are reinforced by SiC particles with pore sizes ranging from 1000 to 1200 μm and produced through liquid-state processing. These composites were rigorously tested and characterized to assess their dry sliding wear behavior [29].

2. Materials and Methods

2.1. Fabrication

The open-cell AlSn6Cu–Al₂O₃ composites were produced using squeeze casting, employing AlSn6Cu aluminum alloy as the matrix and Al₂O₃ particles as the reinforcement. A mixture of Al₂O₃ particles (300–400 μm) and NaCl particles (1000–1200 μm) was used to create the initial salt preform through the replication method [30,31]. After forming, the green compacts were dried at 200 °C for 2 h to remove moisture. Subsequently, the green compacts were sintered at 800 °C \pm 1 °C for 1 h, followed by cooling at room temperature. This process prepared the space holder for infiltration with the AlSn6Cu alloy. The space holder was preheated and placed in a die at 680 °C \pm 2 °C, followed by infiltration using the squeeze casting method at 80 MPa for 60 s. Salt removal was achieved by immersing the composite in an ultrasonic cleaner filled with 79 °C distilled water, resulting in the final open-cell AlSn6Cu–Al₂O₃ skeleton. The alloy, primarily composed of tin (5.5–6.5 wt.%); copper (1.3–1.7 wt.%); and minor additions of nickel (0.2 wt.%), silicon (0.3 wt.%), and other elements, is typically utilized in bearing manufacturing due to its favorable mechanical and wear properties. Tin notably contributes to the formation of a protective layer on bearing surfaces, enhancing lifespan. Al₂O₃ particles were incorporated into the composite to improve tribological performance, selected based on their effectiveness in dry-sliding conditions, with a reinforcement content of 5 wt.% as determined by prior wear behavior studies [29].

In support of the textual description, a schematic illustration of the entire fabrication and characterization process, including the ML analysis for COF prediction, is provided as a flowchart (see Figure 1).

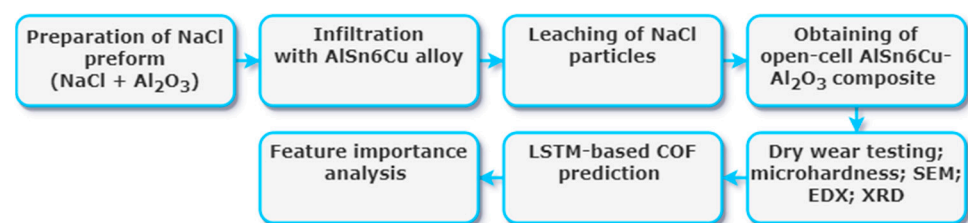


Figure 1. Schematic illustration of the fabrication and characterization processes, along with the ML analysis, for open-cell AlSn6Cu–Al₂O₃ composites.

2.2. Characterization

Within the scope of this research, two distinct sample types were evaluated: an open-cell AlSn6Cu material with a pore size ranging from 1000 to 1200 μm and an open-cell AlSn6Cu–Al₂O₃ composite with pores of the same size. All samples underwent dry wear testing using a TR-20 model Ducom Rotary tribometer (Bangalore, India) operating on a pin-on-disk system. The test samples were spherical-ended, measuring 20 mm in height and 10 mm in diameter, crafted on a lathe, and subjected to wear testing at 1.0 m/s, experiencing two distinct loads, 50 N and 100 N, over a sliding time of 420 s. For these experiments, the counterpart disk was composed of EN-31 steel, with a surface roughness of 1.6 Ra and a hardness of 62 HRC. The steel composition included the following weight percentages: C 0.90 \div 1.20; Si 0.10 \div 0.35 and 0.20; Mn 0.30 \div 0.75; Cr 1.00 \div 1.60; with the remainder being Fe. In each experimental trial, three distinct specimens were subjected to identical testing conditions, with each undergoing a dedicated 420 s wear test. For each specified load condition, whether 50 or 100 N, the testing procedure was replicated with

new samples to maintain the consistency of the testing environment. The data reported in the study represent the mean values derived from these three independent tests, ensuring that the outcomes reflect the average response of the new specimens to the respective load over the 420 s interval. The pin-on-disk test parameters were meticulously selected based on a preliminary study that focused on the wear characterization of an open-cell AlSn6Cu–SiC composite [29]. This foundational research provided critical insights into the optimal testing conditions for evaluating the wear behavior of the composite materials.

The microhardness of the composite's cross-sectional areas was assessed through a light microscope (Polyvar Met, Reichert Jung, Vienna, Austria) equipped with a semi-automated micro-Vickers hardness measurement system (Micro-Duromat 5000 computer control, Reichert Jung, Vienna, Austria). This hardness testing process applied a force of 0.05 kg·f for a duration of 10 s and maintained the pressure for an additional 10 s.

The microstructural features and phase constituents of the open-cell AlSn6Cu–Al₂O₃ composites were determined using SEM and EDX techniques. Sample preparation for these analyses included polishing with varying grits of emery paper and diamond paste, etching with Keller's reagent, and subsequently sputter-coating with a fine gold layer. The SEM imaging was executed using a HIROX SH-5500 scanning electron microscope (SEM, Hirox Japan Co Ltd., Tokyo, Japan), which incorporated a QUANTAX 100 Advanced EDS system (EDS, BRUCKER Co., Frankfurt, Germany). Elemental analysis of the composite matrix and the Al₂O₃ particles was conducted via EDS.

XRD was utilized to identify the distinct phases present in the composite matrix and the Al₂O₃ particles, providing insight into the composite's crystalline structure. The XRD patterns were recorded using a TDM-10 X-ray diffractometer from Dandong Tongda Science and Technology Co., Ltd., Dandong, China, equipped with a scintillation detector. Ni-filtered Cu K α radiation was employed for the diffraction under a tube operating voltage of 35 kV and a current of 30 mA. The diffractograms were obtained in the 2 θ range from 25° to 90°, employing a step size of 0.02° and a scan rate of 0.6°/min, allowing for high-resolution detection of the phases.

2.3. Machine Learning Model

To accurately predict the temporal evolution of the COF for open-cell AlSn6Cu–Al₂O₃ composites and the corresponding unreinforced materials, a LSTM network, which is a specific form of recurrent neural network (RNN) that is capable of capturing long-term dependencies in time series data, was employed. This approach is particularly suitable due to the temporal nature of wear processes, where the history of wear significantly influences future wear behavior [32,33]. The LSTM model is engineered to identify patterns in the COF values over time across different materials, analyzing three samples per material, with the objective of predicting the COF from historical data collected over a span of 420 s. This data was acquired from the experimental methods detailed in Section 2.2, consisting of time series data of COF measured at regular intervals during dry wear friction tests performed using a pin-on-disk apparatus. The primary variable of interest was the COF as a function of time. To prepare these data for model training, the COF values were normalized to the range [0, 1] using the MinMaxScaler, thereby standardizing the scale of the input features. Following normalization, sequences were created with a specified look-back period for the model to learn from, and the data were split into training (70%), validation (15%), and test (15%) sets, which were then reshaped according to the LSTM network's input requirements. The LSTM network architecture comprises a layer with four units, followed by a dense layer for output. After compiling with a mean squared error loss function and optimizing with the Adam optimizer, the model undergoes training on the designated training set. Its performance is subsequently evaluated on both the validation and test sets using key evaluation metrics, including the coefficient of determination (R²), Root Mean Squared Error (RMSE), Mean Absolute Error (MAE), and the Mean Squared Error (MSE). These metrics provide a comprehensive overview of the model's accuracy and predictive power, assessing how effectively the model forecasts COF values against actual observed values.

Through this methodical approach, the LSTM model offers a nuanced prediction of COF values, leveraging historical data collected over a span of 420 s to predict future trends.

To assist in the interpretation of the model's predictive accuracy, plots comparing actual and predicted COF values over time were generated, along with regression plots illustrating the correlation between actual and predicted values for both validation and test datasets. These visualizations not only demonstrated the model's effectiveness but also highlighted areas for potential improvement in future iterations. The deployment of the LSTM network established a robust methodology for predicting the wear characteristics of open-cell AlSn6Cu–Al₂O₃ composites, contributing valuable insights into the material's performance under operational conditions. The ML approach detailed in this study underscores the potential of advanced computational models in enhancing the understanding of material behavior in tribological applications.

Furthermore, an analysis of feature importance was conducted using a Random Forest (RF) algorithm to identify the relative influence of different parameters on the wear behavior [34,35]. The RF, an ensemble learning method comprising multiple decision trees, provides a measure of feature importance that is indicative of the contribution each feature makes to the predictive model's performance [36]. By evaluating the decrease in variance across all trees within the forest attributed to each feature, an importance score is assigned. This score reflects the weight of the feature in the context of the model, with higher values indicating greater influence on the model's predictions. The resulting analysis from the RF regressor, which was trained on the entire dataset, highlighted key factors such as 'load', 'reinforcement', and 'hardness of reinforcement', providing a deeper understanding of their roles in the wear processes of the materials studied.

Figure 2 presents a flowchart that illustrates the comprehensive methodology employed for predicting the COF using LSTM modeling, which details the sequential steps from initial data acquisition through to the feature importance analysis.

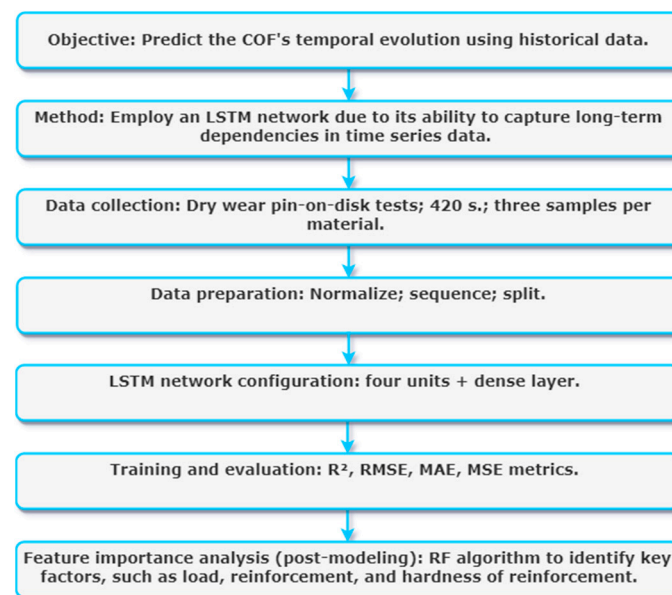


Figure 2. Flowchart illustrating the methodology for predicting COF using LSTM modeling, detailing steps from data acquisition to feature importance analysis.

3. Results and Discussion

3.1. Microstructure

The microstructural analysis of open-cell AlSn6Cu–Al₂O₃ composite post-tribological testing reveals significant insights into the wear mechanisms at play. SEM images at 50 N and 100 N loads (Figure 3a and Figure 3b, respectively) indicate that the wear tracks are characterized by distinct features, such as grooves and debris, which are indicative of

the wear process. EDS analyses conducted on these worn surfaces provide a quantitative measure of the elemental composition in different zones, which are marked as 1 and 2 in the SEM images. In both SEM images, zones marked as '1' are visible parts of Al_2O_3 particles, which act as reinforcements in the cell wall.

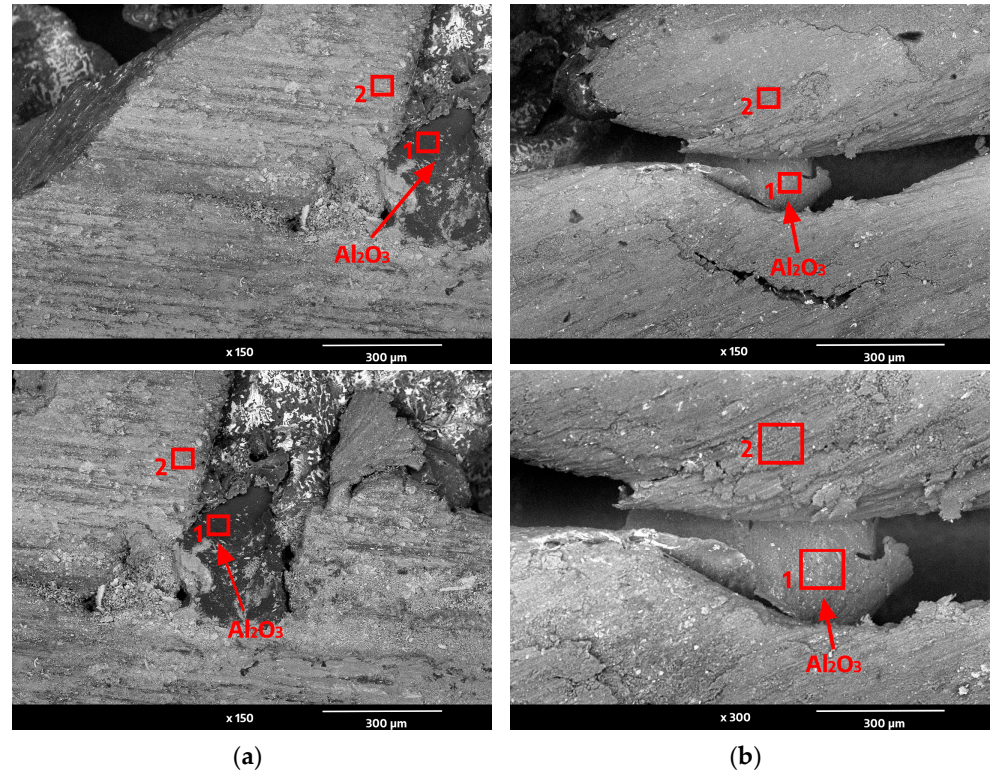


Figure 3. SEM images of AlSn6Cu– Al_2O_3 composites showing microstructural details under different applied loads: (a) 50 N; (b) 100 N.

At 50 N load, the EDS analysis of zone 1 (Table 1) shows a higher Al content of 65.45% and oxygen content of 33.83%, suggesting that the cell wall contains Al_2O_3 reinforcement particles. Zone 2 (Table 1) reveals a substantial increase in Fe content to 60.01%, alongside a decrease in Al content to 29.91%, hinting at the occurrence of adhesive wear, characterized by material transfer from the counterface to an upper layer of the composite distant from the cell wall. The presence of Sn and Cu in zone 2 (Table 1) can be associated with the composite constituents being exposed or redistributed due to wear, also suggesting abrasive wear where the counterface or entrapped particles may have abraded the surface of the composite.

Table 1. EDS analysis of the contact surface of AlSn6Cu– Al_2O_3 composite after tribological tests with a 50 N of load, relating to specific areas indicated in Figure 3a.

| Analysis № | Al | Fe | O | Sn | Cu |
|------------|-------|-------|-------|------|------|
| 1 | 65.45 | 0.72 | 33.83 | - | - |
| 2 | 29.91 | 60.01 | 7.32 | 2.26 | 0.49 |

Under the increased load of 100 N, the EDS analysis in zone 1 (Table 2) shows a slight decrease in Al content to 58.03% and an increase in oxygen content to 35.85%, indicating more substantial wear at this load but still showcasing evidence for Al_2O_3 reinforcement particles within the cell wall structure. The marginal increase in Fe content to 6.11% could be a sign of increased adhesive wear due to more significant mechanical interaction. Zone 2 (Table 2) under this higher load condition shows an increase in Fe content to 31.03%, and the presence of Sn and Cu to 3.68% and 0.90%, respectively, could indicate a more

pronounced degree of abrasive wear, as well as mechanical mixing between the composite and counterface materials.

Table 2. EDS analysis of the contact surface of AlSn6Cu–Al₂O₃ composite after tribological tests with a 100 N of load, relating to specific areas indicated in Figure 3b.

| Analysis № | Al | Fe | O | Sn | Cu |
|------------|-------|-------|-------|------|------|
| 1 | 58.03 | 6.11 | 35.85 | - | - |
| 2 | 52.95 | 31.03 | 11.44 | 3.68 | 0.90 |

These variations in elemental composition with the increasing load from 50 N to 100 N reflect a transition from mild wear conditions where adhesive wear dominates to more severe conditions where abrasive wear and mechanical mixing become more pronounced. The increase in Fe, Sn, and Cu content at higher loads suggests that both adhesive and abrasive wear mechanisms contribute to the wear of the composites. Adhesive wear is evident from the material transfer, where increased Fe content indicates more interaction with the steel counterface. Abrasive wear is suggested by the presence of grooves and debris, especially at higher loads where there is likely to be more significant abrasion from the counterface. The SEM images and EDS analysis correlate well with the expected behaviors of such composites under tribological stress, displaying a combination of wear mechanisms responsible for material degradation.

The role of Al₂O₃ as reinforcement is evident. It aids in reducing direct metal-to-metal contact during sliding under both loads. The Al₂O₃ particles also act as a solid lubricant, which may prevent direct contact between the surfaces of the matrix and the counterbody in the contact zone. The wear resistance of the open-cell composites depends on the load, as Kolev et al. indicated [37], and on the incorporation of reinforcement particles that act as solid lubricants in the contact zone during friction [38] and that strengthen the cell walls of the composite when it is under load during the wear process [7].

Figure 4a presents the XRD pattern of an AlSn6Cu–Al₂O₃ composite before the initiation of wear testing. The diffractogram exhibits distinct peaks corresponding to the composite's constituent phases. Sharp and well-defined peaks characteristic of the Al_{1-x}(Cu,Sn)_x phase are observed at 2θ values of approximately [39.0; 45.1; 65.6; 78.8], indicative of its crystalline nature. Similarly, the presence of Sn is confirmed by peaks at approximately [31.1; 32.4; 44.3; 55.7; 63.0; 72.8; 73.5; 79.9]. The Al₂O₃ phase is also identified with less intense peaks at approximately [35.5; 37.5; 43.7; 52.2; 57.9; 65.0], which may be due to its dispersion within the composite. Additionally, Figure 4b depicts the XRD pattern of an AlSn6Cu material. This pattern similarly shows sharp peaks associated with Al_{1-x}(Cu,Sn)_x and Sn phases, without the peaks corresponding to Al₂O₃ observed in Figure 4a.

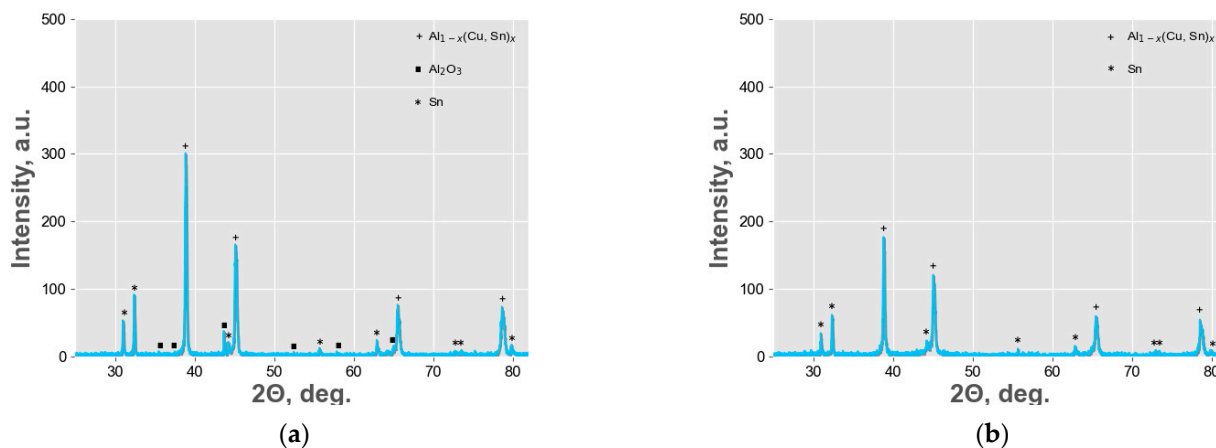


Figure 4. XRD patterns of the materials prior to wear testing: (a) AlSn6Cu–Al₂O₃ composite; (b) AlSn6Cu.

3.2. Micro-Hardness and Wear Behavior

The average Vickers hardness (HV) was tested using a force of 0.05 kg·f applied for 10 s and maintained for an additional 10 s. The micro-hardness analysis, as depicted in Figure 5, illustrates a significant disparity in hardness between the matrix and the reinforcement. The reinforcement displayed a notably higher hardness (2287.92 HV) compared to the matrix (61.46 HV), which is a staggering increase of approximately 3621%. This vast difference in hardness can be attributed to the reinforcement particles, which provide more support and strengthen the cell walls of the composite when it is under load during friction. The micro-hardness results are consistent with those from the study on open-cell AlSn6Cu composites reinforced with SiC particles, where the micro-hardness values of the matrix are 62.62 and those of the reinforcement are 2418.74 [29].

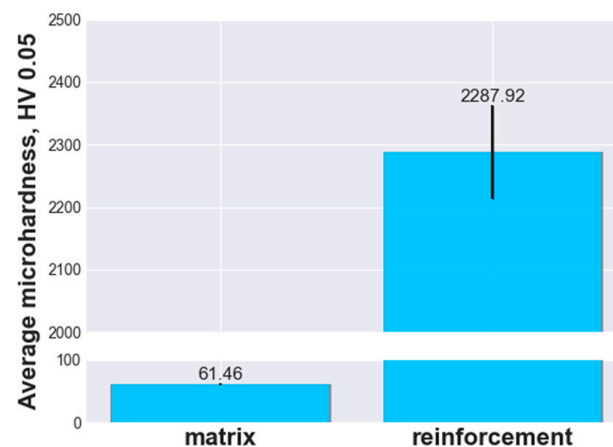


Figure 5. Microhardness analysis of open-cell AlSn6Cu–Al₂O₃ composites.

The pin-on-disk tests were performed with a linear velocity of 1.0 m/s, experiencing two distinct loads, 50 N and 100 N, across a sliding time of 420 s. In Figure 5, the COF shows a gradual increase with the applied load for both materials. The COF for the unreinforced material increased from 0.46 at 50 N to 0.48 at 100 N—a relative increase of about 4.34%. The reinforced composite experienced a similar incremental trend from 0.49 at 50 N to 0.51 at 100 N, which is an increase of approximately 4.08%. This indicates that the COF is marginally sensitive to the increase in load, with the reinforced composite maintaining a slightly higher COF under both loading conditions. A quantitative comparison of the COF values between the open-cell AlSn6Cu matrix material and the open-cell AlSn6Cu–Al₂O₃ composite shows that the difference is small and falls in the measurement error. The percentage difference between the COF values of the two materials is about 6.52% at 50 N and 6.25% at 100 N, which indicates that the open-cell AlSn6Cu–Al₂O₃ composite has slightly higher friction than the open-cell AlSn6Cu matrix material under both loads. The larger standard deviation observed in the COF at 50 N load, as presented in Figure 6, can be attributed to the nonuniform distribution of the Al₂O₃ reinforcement particles and the heterogeneity of the cell walls, which are in the range of 1000–1200 μm, within both materials. The results could be explained by the appearance of the Al₂O₃ particles in the contact zone, which increases the friction by increasing the temperature, the surface roughness, and the contact area. The results for both materials of the COF are consistent with the results of the study of open-cell AlSn6Cu composites reinforced with SiC particles and tested at loads of 50 N and 100 N in dry friction conditions [29].

Furthermore, the mass wear depicted in Figure 7 also demonstrates a dependency on the load and reinforcement. The unreinforced material showed a substantial increase in wear from 8.05 mg at 50 N to 17.55 mg at 100 N. The reinforced composite also exhibited an increase in wear from 1.90 mg at 50 N to 8.10 mg at 100 N. The substantial standard deviation in mass wear at the 100 N load, as observed in Figure 6, reflects the impact of the nonuniform distribution of the Al₂O₃ reinforcement particles and the heterogeneity of the

cell walls. A quantitative comparison of the mass wear values between the unreinforced and the reinforced materials shows a significant decrease in the mass wear by 76.39% at 50 N and 53.85% for the open-cell AlSn6Cu–Al₂O₃ composite. This dramatic decrease in mass wear for the reinforced composite under both loads suggests that the Al₂O₃ particles act as a barrier against the wear process, preventing the removal of material from the cell walls and reducing the wear rate, which is also reported in Refs. [37,39,40].

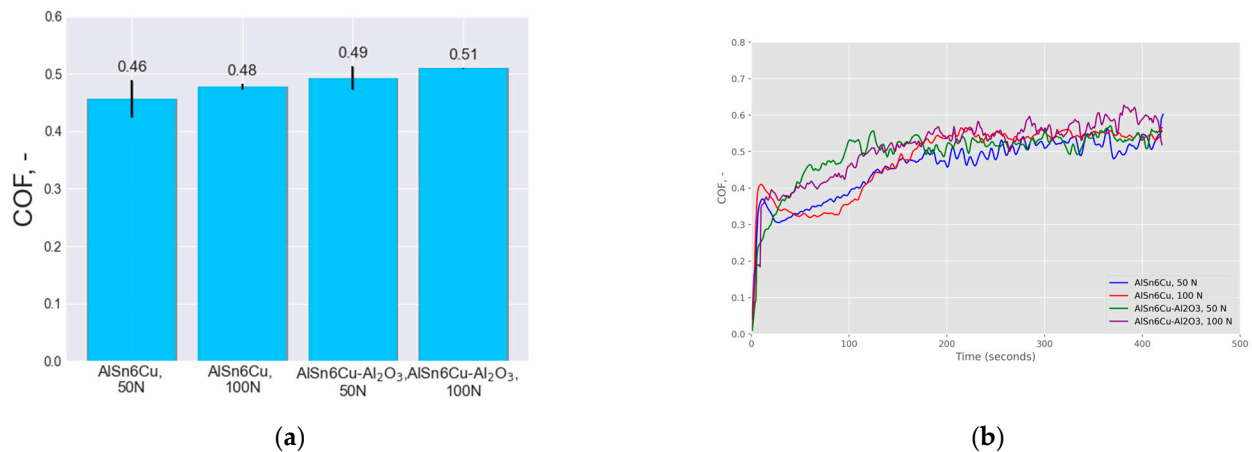


Figure 6. Comparative analysis of COF in open-cell AlSn6Cu–Al₂O₃ composites and open-cell unreinforced materials tested at 50 N and 100 N: (a) bar plot; (b) COF curves.

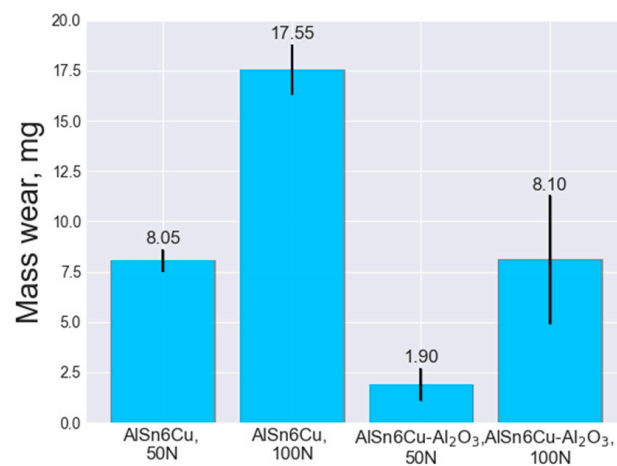


Figure 7. Bar plot depicting the mass wear (mg) of open-cell AlSn6Cu–Al₂O₃ composites and open-cell unreinforced materials tested at 50 N and 100 N.

3.3. COF Prediction and Model Performance Evaluation

Figure 8 presents a comprehensive comparison between actual and predicted COF values over time for both AlSn6Cu material and AlSn6Cu–Al₂O₃ composites under two distinct test conditions. Figure 8a,b illustrates the performance at a 50 N load, showcasing the predictive accuracy of the unreinforced AlSn6Cu material and the AlSn6Cu–Al₂O₃ composite, respectively. Similarly, Figure 8c,d display the outcomes at a 100 N load, providing insight into the model's predictive capability for the same materials under increased load. These visualizations underscore the effectiveness of the LSTM model in capturing the nuanced wear behaviors of both materials across varying operational conditions, highlighting its potential utility in predictive maintenance and material design optimization.

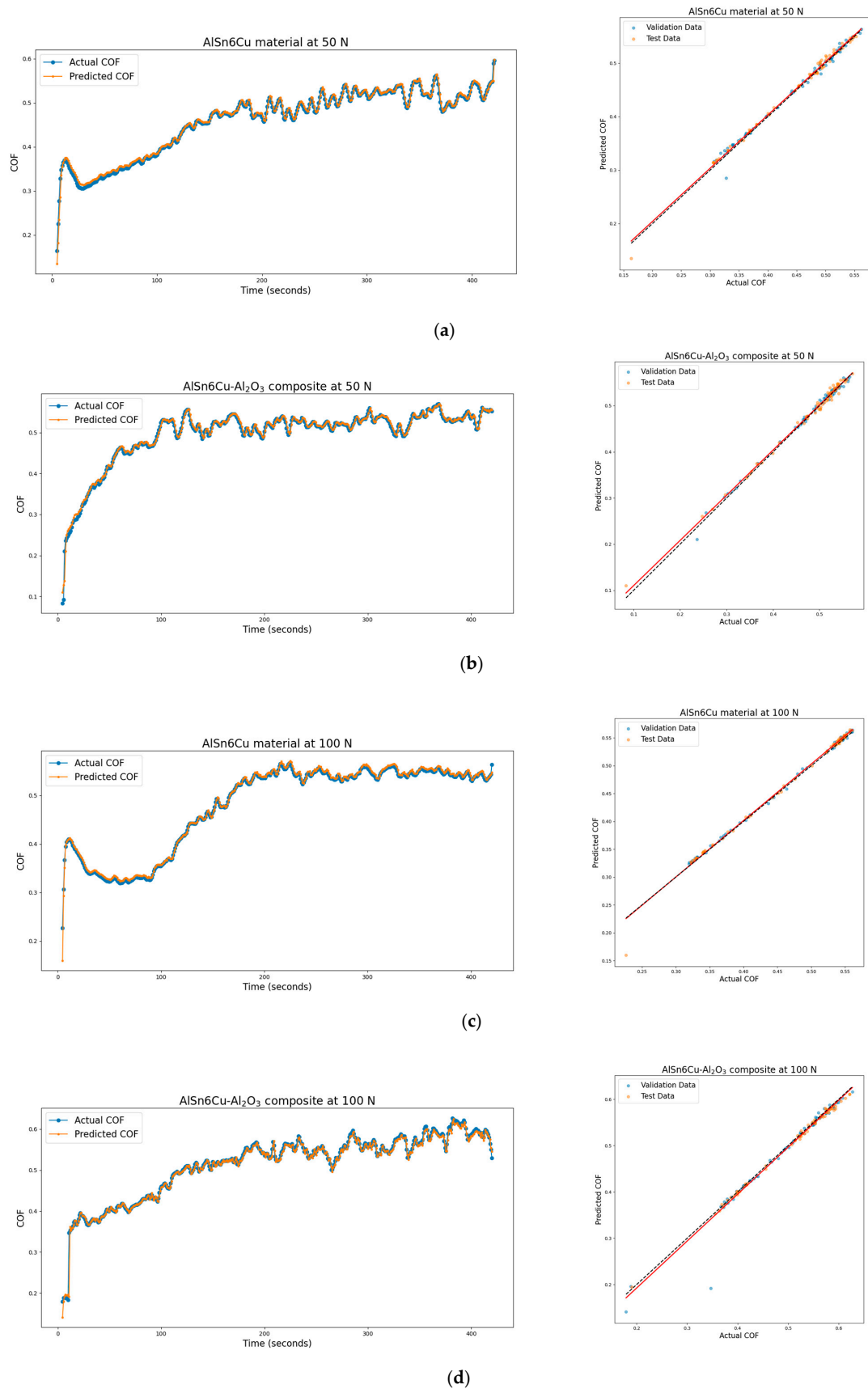


Figure 8. Comparative analysis of actual vs. predicted COF under different applied loads: (a) AlSn6Cu material at 50 N; (b) AlSn6Cu–Al₂O₃ composite at 50 N; (c) AlSn6Cu material at 100 N; (d) AlSn6Cu–Al₂O₃ composite at 100 N.

To quantitatively assess the performance of the LSTM model, its effectiveness was evaluated across various metrics (MSE, RMSE, MAE, R^2). These metrics were calculated for both validation and test datasets across all experimental conditions and materials tested. Table 3 summarizes these findings, offering a nuanced view of the model's predictive performance. The descriptive statistics for the COF values across different materials and test conditions were systematically analyzed and presented in Table 4, revealing the inherent variability in the experimental data. The LSTM model showcased remarkable predictive accuracy across all conditions, with the test R^2 values being consistently high. In particular, for the AlSn6Cu–Al₂O₃ composite at 100 N, characterized by a mean of 0.50967 and a standard deviation of 0.08644, the R^2 value improved from 0.95585 in the validation set to 0.99638 in the test set. Meanwhile, for the composite at 50 N, which had a mean of 0.49294 and a standard deviation of 0.08060, the R^2 value experienced a slight decrease from 0.99388 in the validation set to 0.99303 in the test set. The performance metrics also reveal how material composition and load conditions affect predictive accuracy. For instance, the AlSn6Cu material at 100 N with a mean of 0.47711 and a standard deviation of 0.09410 showed an exceptionally high validation R^2 of 0.99810, suggesting near-perfect prediction under higher load conditions. This contrasts with its performance at 50 N, where a slight decrease in R^2 to 0.98978 was observed, still indicating very high predictive accuracy but showcasing sensitivity to changes in testing conditions.

Table 3. Evaluation metrics for LSTM model predictions for open-cell AlSn6Cu–Al₂O₃ composite and open-cell AlSn6Cu material under different applied loads.

| Analysis | Dataset | MSE | RMSE | MAE | R^2 |
|---|------------|---------|-----------|-----------|---------|
| AlSn6Cu–Al ₂ O ₃ at 100 N | Validation | 0.00039 | 0.0198000 | 0.0066391 | 0.95585 |
| AlSn6Cu–Al ₂ O ₃ at 100 N | Test | 0.00003 | 0.0053078 | 0.0041946 | 0.99638 |
| AlSn6Cu–Al ₂ O ₃ at 50 N | Validation | 0.00004 | 0.0061351 | 0.0046952 | 0.99388 |
| AlSn6Cu–Al ₂ O ₃ at 50 N | Test | 0.00005 | 0.0073764 | 0.0056358 | 0.99303 |
| AlSn6Cu at 100 N | Validation | 0.00002 | 0.0040804 | 0.0035303 | 0.99810 |
| AlSn6Cu at 100 N | Test | 0.00008 | 0.0091727 | 0.0043677 | 0.99056 |
| AlSn6Cu at 50 N | Validation | 0.00007 | 0.0081300 | 0.0052856 | 0.98978 |
| AlSn6Cu at 50 N | Test | 0.00004 | 0.006027 | 0.0046216 | 0.99494 |

Table 4. Descriptive statistics of COF for open-cell AlSn6Cu–Al₂O₃ composite and open-cell AlSn6Cu material under different applied loads.

| Analysis | Mean | Std | Min | 25% | 50% | 75% | Max |
|---|---------|---------|---------|---------|---------|---------|---------|
| AlSn6Cu–Al ₂ O ₃ at 100 N | 0.50967 | 0.08644 | 0.04160 | 0.46471 | 0.53642 | 0.56443 | 0.62715 |
| AlSn6Cu–Al ₂ O ₃ at 50 N | 0.49294 | 0.08060 | 0.00990 | 0.49220 | 0.51990 | 0.53380 | 0.57070 |
| AlSn6Cu at 100 N | 0.47711 | 0.09410 | 0.01805 | 0.39445 | 0.53505 | 0.54580 | 0.56715 |
| AlSn6Cu at 50 N | 0.45710 | 0.08162 | 0.01520 | 0.39882 | 0.48275 | 0.51697 | 0.60240 |

3.4. Feature Importance Analysis for Mass Wear and COF Prediction

The predictive models for mass wear and COF in tribological systems rely heavily on understanding which factors significantly influence wear behavior. Through the use of a RF regressor, a feature importance analysis was conducted (Figure 9) to identify the relative importance of various factors contributing to COF (Figure 9a) and mass wear (Figure 9b) in open-cell AlSn6Cu–Al₂O₃ composites.

The analysis revealed that 'load' is the most influential factor for both COF and mass wear, with importance scores of 0.65 and 0.47, respectively. This underscores the critical role that mechanical stress plays in the wear mechanisms of the composites. 'Reinforcement' emerged as the second most significant feature, with scores of 0.20 for COF and 0.32 for mass wear, indicating that the presence of reinforcing elements is a key determinant in the wear resistance of the material.

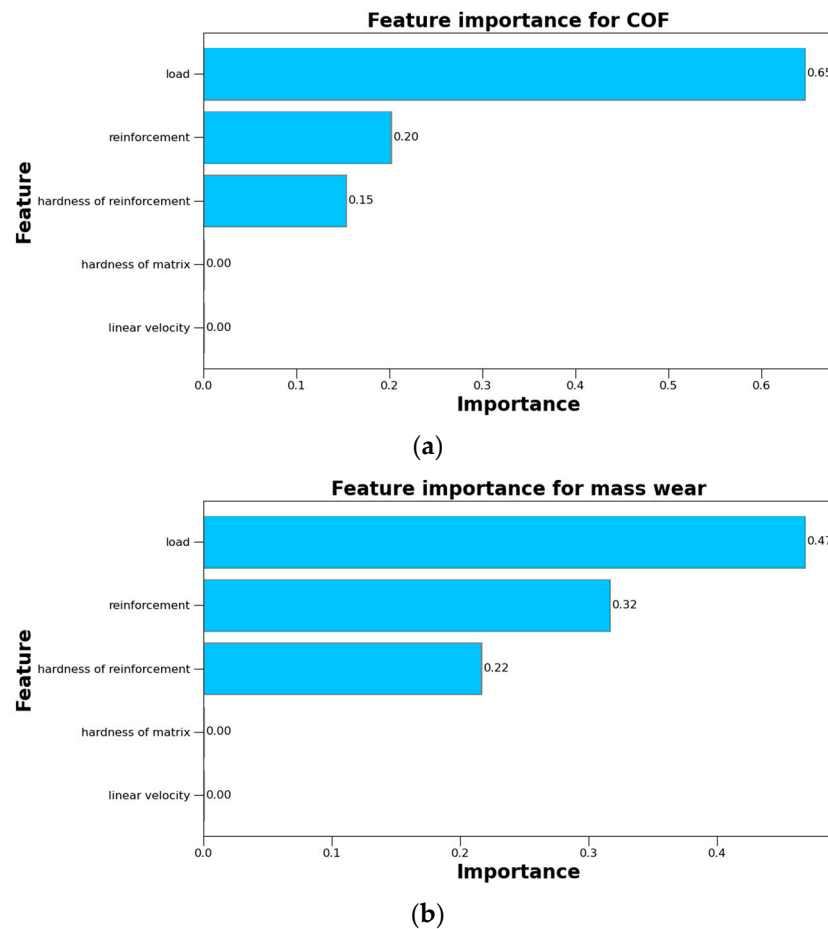


Figure 9. Feature importance plots derived from RF regression analysis for open-cell AlSn6Cu–Al₂O₃ composites, showing the relative contributions of various parameters to: (a) COF; (b) mass wear.

‘Hardness of reinforcement’ also showed a considerable impact on the wear properties, with feature importance scores of 0.15 for COF and 0.22 for mass wear. This finding aligns with the understanding that harder reinforcement materials can improve the composite’s wear resistance. Interestingly, ‘hardness of matrix’ and ‘linear velocity’ were found to have no discernible effect on the prediction of both COF and mass wear in this specific analysis, receiving scores of 0.00.

The importance plots illustrate these findings graphically, providing a clear and immediate visual representation of the factors that most significantly affect wear and friction in these composites. The results not only guide the design and material selection for improved wear performance but also enhance the understanding of the wear process under different operating conditions.

4. Conclusions

This comprehensive study on the fabrication and wear characterization of open-cell AlSn6Cu–Al₂O₃ composites, reinforced with the aid of advanced LSTM-based modeling for the prediction of the COF, marks a significant advancement in the field of AMMCs. Through the utilization of liquid-state processing techniques and meticulous empirical analysis, this research not only fortifies the foundational knowledge of AMMCs but also showcases the potential of integrating ML to bridge the gap between computational predictions and real-world applications.

The open-cell AlSn6Cu–Al₂O₃ composites demonstrated distinct microstructural qualities, with SEM, EDS, and XRD analyses confirming the presence of Al₂O₃ particles within the cell walls, which were pivotal in wear resistance. Notably, at the 50 N load, the reinforced composites showcased a small COF increment from 0.46 to 0.49 and a remarkable

reduction in mass wear from 8.05 mg to 1.90 mg. As the load increased to 100 N, the reinforced composites showed a slight COF increment from 0.48 to 0.51 and a big reduction in mass wear from 17.55 mg to 8.10 mg. These quantitative improvements highlight the reinforced composite's ability to endure and resist wear even under elevated mechanical stress. The reinforcement of Al₂O₃ within the composite's cell walls proved to be crucial in enhancing the wear resistance by performing as a solid lubricant.

Moreover, the application of the LSTM neural network model accurately predicted the temporal changes in COF, demonstrating exceptional performance across various metrics. The feature importance analysis further elucidated the significant impact of 'load' and 'reinforcement' on the wear process, with 'hardness of reinforcement' also playing a substantial role in dictating the wear properties of the composites.

This study demonstrates a pioneering integration of ML with materials science to predict wear characteristics in open-cell AMMCs, with significant potential for creating cost-effective, wear-resistant materials for high-performance applications, and future efforts will aim to enhance these models and expand empirical studies across a wider range of composites and operational conditions.

Author Contributions: Conceptualization, M.K. and L.D.; methodology, M.K., V.P., R.D. and K.K.; software, M.K., V.P., R.D. and K.K.; formal analysis, M.K., V.P., R.D., T.S. and K.K.; investigation, M.K., V.P., R.D. and K.K.; resources, L.D.; writing—original draft preparation, M.K.; writing—review and editing, M.K.; visualization, M.K.; supervision, M.K. and L.D.; project administration, M.K. and T.S.; funding acquisition, M.K. and T.S. All authors have read and agreed to the published version of the manuscript.

Funding: This research was funded by the Bulgarian National Science Fund, Project KII-06-H57/20 'Fabrication of new type of self-lubricating antifriction metal matrix composite materials with improved mechanical and tribological properties'.

Institutional Review Board Statement: Not applicable.

Informed Consent Statement: Not applicable.

Data Availability Statement: The raw data supporting the conclusions of this article will be made available by the authors on request.

Acknowledgments: We acknowledge the support of the European Regional Development Fund within the OP Science and Education for Smart Growth 2014–2020, Project CoE, National Center of Mechatronics and Clean Technologies, BG05M2OP001-1.001-0008, in providing the necessary equipment for conducting the SEM, EDS, and XRD analyses in this work.

Conflicts of Interest: The authors declare no conflicts of interest.

References

1. Chelladurai, S.J.S.; Kumar, S.S.; Venugopal, N.; Ray, A.P.; Manjunath, T.C.; Gnanasekaran, S. A Review on Mechanical Properties and Wear Behaviour of Aluminium Based Metal Matrix Composites. *Mater. Today Proc.* **2021**, *37*, 908–916. [\[CrossRef\]](#)
2. Nturanabo, F.; Masu, L.; Kirabira, J. Novel Applications of Aluminium Metal Matrix Composites. In *Aluminium Alloys and Composites*; BoD—Books on Demand: Norderstedt, Germany, 2019. [\[CrossRef\]](#)
3. Chak, V.; Chattopadhyay, H.; Dora, T.L. A Review on Fabrication Methods, Reinforcements and Mechanical Properties of Aluminum Matrix Composites. *J. Manuf. Process.* **2020**, *56*, 1059–1074. [\[CrossRef\]](#)
4. Stanev, L.; Kolev, M.; Drenchev, B.; Drenchev, L. Open-Cell Metallic Porous Materials Obtained Through Space Holders—Part II: Structure and Properties. A Review. *J. Manuf. Sci. Eng.* **2016**, *139*, 050802. [\[CrossRef\]](#)
5. Garg, P.; Jamwal, A.; Kumar, D.; Sadasivuni, K.K.; Hussain, C.M.; Gupta, P. Advance Research Progresses in Aluminium Matrix Composites: Manufacturing & Applications. *J. Jpn. Res. Inst. Adv. Copper-Base Mater. Technol.* **2019**, *8*, 4924–4939. [\[CrossRef\]](#)
6. Wan, T.; Liu, Y.; Zhou, C.; Chen, X.; Li, Y. Fabrication, Properties, and Applications of Open-Cell Aluminum Foams: A Review. *J. Mater. Sci.* **2021**, *62*, 11–24. [\[CrossRef\]](#)
7. Kolev, M.; Drenchev, L.; Simeonova, T.; Krastev, R.; Kavardzhikov, V. Data on Mechanical Properties of Open-Cell AlSi₁₀Mg Materials and Open-Cell AlSi₁₀Mg-SiC Composites with Different Pore Sizes and Strain Rates. *Data Brief* **2023**, *49*, 109461. [\[CrossRef\]](#)
8. Bhardwaj, A.R.; Vaidya, A.M.; Shekhawat, S.P. Machining of Aluminium Metal Matrix Composite: A Review. *Mater. Today Proc.* **2020**, *21*, 1396–1402. [\[CrossRef\]](#)

9. Shyha, I.; Huo, D. *Advances in Machining of Composite Materials: Conventional and Non-Conventional Processes*; Springer Nature: Berlin/Heidelberg Germany, 2021; ISBN 9783030714383.
10. Schmidt, A.; Siebeck, S.; Götze, U.; Wagner, G.; Nestler, D. Particle-Reinforced Aluminum Matrix Composites (AMCs)—Selected Results of an Integrated Technology, User, and Market Analysis and Forecast. *Metals* **2018**, *8*, 143. [[CrossRef](#)]
11. Venkatesh, R.; Sethi, D.; Kolli, V.; Saha Roy, B. Experimental Investigation of Aluminium Matrix Composite Production and Joining. *Mater. Today* **2019**, *18*, 5276–5285. [[CrossRef](#)]
12. Suthar, J.; Patel, K.M. Processing Issues, Machining, and Applications of Aluminum Metal Matrix Composites. *Mater. Manuf. Process.* **2018**, *33*, 499–527. [[CrossRef](#)]
13. Luo, Y.; Yu, S.; Liu, J.; Zhu, X.; Luo, Y. Compressive Property and Energy Absorption Characteristic of Open-Cell SiCp/AlSi₉Mg Composite Foams. *J. Alloys Compd.* **2010**, *499*, 227–230. [[CrossRef](#)]
14. Monno, M.; Negri, D.; Mussi, V.; Aghaei, P.; Groppi, G.; Tronconi, E.; Strano, M. Cost-Efficient Aluminum Open-Cell Foams: Manufacture, Characterization, and Heat Transfer Measurements. *Adv. Eng. Mater.* **2018**, *20*, 1701032. [[CrossRef](#)]
15. Duarte, I.; Vesjenjak, M.; Krstulović-Opara, L.; Ren, Z. Crush Performance of Multifunctional Hybrid Foams Based on an Aluminium Alloy Open-Cell Foam Skeleton. *Polym. Test.* **2018**, *67*, 246–256. [[CrossRef](#)]
16. Rusin, N.M.; Skorentsev, A.L.; Krinitsyn, M.G. Relationship between Wear Resistance under Dry Friction and Mechanical Properties of Sintered Al–Sn Composites. *Inorg. Mater. Appl. Res.* **2021**, *12*, 776–784. [[CrossRef](#)]
17. Rusin, N.M.; Skorentsev, A.L.; Krinitsyn, M.G.; Dmitriev, A.I. Tribotechnical Properties of Sintered Antifriction Aluminum-Based Composite under Dry Friction against Steel. *Materials* **2021**, *15*, 180. [[CrossRef](#)] [[PubMed](#)]
18. Rusin, N.M.; Skorentsev, A.L. Mechanical and Tribological Properties of Sintered Aluminum Matrix Al–Sn Composites Reinforced with Al₃Fe Particles. *Phys. Met. Metall.* **2021**, *122*, 1248–1255. [[CrossRef](#)]
19. Rusin, N.M.; Skorentsev, A.L.; Dmitriev, A.I. Effect of the Reinforcing Particle Introduction Method on the Tribomechanical Properties of Sintered Al–Sn–Fe Alloys. *Metals* **2023**, *13*, 1483. [[CrossRef](#)]
20. Bertelli, F.; Freitas, E.S.; Cheung, N.; Arenas, M.A.; Conde, A.; de Damborenea, J.; Garcia, A. Microstructure, Tensile Properties and Wear Resistance Correlations on Directionally Solidified Al–Sn–(Cu; Si) Alloys. *J. Alloys Compd.* **2017**, *695*, 3621–3631. [[CrossRef](#)]
21. Banerjee, T.; Dey, S.; Sekhar, A.P.; Datta, S.; Das, D. Design of Alumina Reinforced Aluminium Alloy Composites with Improved Tribo-Mechanical Properties: A Machine Learning Approach. *Trans. Indian Inst. Met.* **2020**, *73*, 3059–3069. [[CrossRef](#)]
22. Wang, Y.; Soutis, C.; Ando, D.; Sutou, Y.; Narita, F. Application of Deep Neural Network Learning in Composites Design. *Eur. J. Mater.* **2022**, *2*, 117–170. [[CrossRef](#)]
23. Thankachan, T.; Soorya Prakash, K.; Malini, R.; Ramu, S.; Sundararaj, P.; Rajandran, S.; Rammasamy, D.; Jothi, S. Prediction of Surface Roughness and Material Removal Rate in Wire Electrical Discharge Machining on Aluminum Based Alloys/Composites Using Taguchi Coupled Grey Relational Analysis and Artificial Neural Networks. *Appl. Surf. Sci.* **2019**, *472*, 22–35. [[CrossRef](#)]
24. Idrisi, A.H.; Hamid Ismail Mourad, A. Wear Performance Analysis of Aluminum Matrix Composites Using Artificial Neural Network. In Proceedings of the 2019 Advances in Science and Engineering Technology International Conferences (ASET), Dubai, United Arab Emirates, 26 March–10 April 2019.
25. Wiciak-Pikuła, M.; Felusiak-Czyryca, A.; Twardowski, P. Tool Wear Prediction Based on Artificial Neural Network during Aluminum Matrix Composite Milling. *Sensors* **2020**, *20*, 5798. [[CrossRef](#)] [[PubMed](#)]
26. Mishra, A.; Jatti, V.S. Prediction of Wear Rate in Al/SiC Metal Matrix Composites Using a Neurosymbolic Artificial Intelligence (NSAI)-Based Algorithm. *Lubricants* **2023**, *11*, 261. [[CrossRef](#)]
27. Agme, V.N.; Ashish; Pant, R.; Sridevi, M.; Suman, A.; Vijaya Sekhar Babu, M. Analysis and Prediction of Wear Characteristics of Sustainable Metal Matrix Composites Using Machine Learning with Decision Making Algorithm. In Proceedings of the 2023 4th International Conference on Smart Electronics and Communication (ICOSEC), Trichy, India, 20–22 September 2023; pp. 1401–1407.
28. Hasan, M.S.; Kordijazi, A.; Rohatgi, P.K.; Nosonovsky, M. Triboinformatic Modeling of Dry Friction and Wear of Aluminum Base Alloys Using Machine Learning Algorithms. *Tribol. Int.* **2021**, *161*, 107065. [[CrossRef](#)]
29. Kolev, M.; Drenchev, L.; Petkov, V.; Dimitrova, R.; Kovacheva, D. Open-Cell AlSn₆Cu–SiC Composites: Fabrication, Dry-Sliding Wear Behavior, and Machine Learning Methods for Wear Prediction. *Materials* **2023**, *16*, 6208. [[CrossRef](#)] [[PubMed](#)]
30. Łazińska, M.; Durejko, T.; Lipiński, S.; Polkowski, W.; Czujko, T.; Varin, R.A. Porous Graded FeAl Intermetallic Foams Fabricated by Sintering Process Using NaCl Space Holders. *Mater. Sci. Eng. A* **2015**, *636*, 407–414. [[CrossRef](#)]
31. Lefebvre, L.-P.; Banhart, J.; Dunand, D.C. Porous Metals and Metallic Foams: Current Status and Recent Developments. *Adv. Eng. Mater.* **2008**, *10*, 775–787. [[CrossRef](#)]
32. Zhang, F.; Wang, L.; Ye, W.; Li, Y.; Yang, F. Ultrasonic Lamination Defects Detection of Carbon Fiber Composite Plates Based on Multilevel LSTM. *Compos. Struct.* **2024**, *327*, 117714. [[CrossRef](#)]
33. Zhao, Y.; Chen, Z.; Dong, Y.; Tu, J. An Interpretable LSTM Deep Learning Model Predicts the Time-Dependent Swelling Behavior in CERCER Composite Fuels. *Mater. Today Commun.* **2023**, *37*, 106998. [[CrossRef](#)]
34. Zhao, Y.; Zhu, W.; Wei, P.; Fang, P.; Zhang, X.; Yan, N.; Liu, W.; Zhao, H.; Wu, Q. Classification of Zambian Grasslands Using Random Forest Feature Importance Selection during the Optimal Phenological Period. *Ecol. Indic.* **2022**, *135*, 108529. [[CrossRef](#)]
35. Alsagri, H.S.; Ykhlef, M. Quantifying Feature Importance for Detecting Depression Using Random Forest. *Int. J. Adv. Comput. Sci. Appl.* **2020**, *11*. [[CrossRef](#)]

36. Wu, D.; Jennings, C.; Terpenney, J.; Gao, R.X.; Kumara, S. A Comparative Study on Machine Learning Algorithms for Smart Manufacturing: Tool Wear Prediction Using Random Forests. *J. Manuf. Sci. Eng.* **2017**, *139*, 071018. [[CrossRef](#)]
37. Kolev, M.; Drenchev, L.; Petkov, V.; Dimitrova, R. Production and Tribological Characterization of Advanced Open-Cell AlSi₁₀Mg-Al₂O₃ Composites. *Metals* **2023**, *13*, 131. [[CrossRef](#)]
38. Kolev, M.; Drenchev, L.; Petkov, V. Fabrication, Experimental Investigation and Prediction of Wear Behavior of Open-Cell AlSi₁₀Mg-SiC Composite Materials. *Metals* **2023**, *13*, 814. [[CrossRef](#)]
39. Bharath, V.; Nagaral, M.; Auradi, V.; Kori, S.A. Preparation of 6061Al-Al₂O₃ MMC's by Stir Casting and Evaluation of Mechanical and Wear Properties. *Procedia Mater. Sci.* **2014**, *6*, 1658–1667. [[CrossRef](#)]
40. Ghanaraja, S.; Ravikumar, K.S.; Raju, H.P.; Madhusudan, B.M. Studies on Dry Sliding Wear Behaviour of Al₂O₃ Reinforced Al Based Metal Matrix Composites. *Mater. Today* **2017**, *4*, 10043–10048. [[CrossRef](#)]

Disclaimer/Publisher's Note: The statements, opinions and data contained in all publications are solely those of the individual author(s) and contributor(s) and not of MDPI and/or the editor(s). MDPI and/or the editor(s) disclaim responsibility for any injury to people or property resulting from any ideas, methods, instructions or products referred to in the content.